JOURNAL OF MATERIALS SCIENCE 17 (1982) 893–900

Kinking and compressive failure in uniaxially aligned carbon fibre composite tested under superposed hydrostatic pressure

T. V. PARRY, A. S. WRONSKI
School of Materials Science, University of Bradford, Bradford, West Yorkshire, UK

Initiation and propagation of failure in uniaxially aligned 60% volume-fraction Type III carbon fibre–epoxide compressive specimens, strained parallel to the fibre axis, was studied at atmospheric and superposed hydrostatic pressures, H, extending to 300 MN m^{-2}. The atmospheric axial compressive strength was approximately 1.5 GN m^{-2} and equal to the tensile strength, but mechanisms involving shear-operated failure of the fibres must be discounted since the failure process was very pressure sensitive above $H \sim 150$ MN m^{-2}. The results also could not be satisfactorily interpreted by theories involving micro-buckling of individual fibres or laminae when the matrix shear modulus controls the compressive strength. For atmospheric tests and for $H < 150$ MN m^{-2} the initiation of failure was associated with transverse cracking (longitudinal splitting) which was followed by kinking. Ahead of the propagating kink band, groups of fractured fibres were observed, which is consistent with failure of these groups by buckling; this process causes composite catastrophic failure. At higher pressures splitting was suppressed, as was interlaminar cracking in doubly-notched (in-plane shear) specimens, but kinking, which became increasingly more difficult to initiate, was the precursor of the failure process. An attempt was made to analyse failure using the fracture mechanics model of Chaplin with some success for the notched specimens.

1. Introduction

Previous studies of the compressive strength of uniaxially aligned fibrous composites have shown different types of deformation and failure behaviour, usually described as "shear" [1–5], "interfacial" [6], "splitting" [7], "fibre buckling" [8, 9] and "kinking" [7, 10–12]. Failure mode has been demonstrated to vary with temperature [13] fibre volume-fraction, V_f, [14] specimen shape [14] and, probably, testing jig [14]. For carbon fibre-reinforced resins (CFRP) having a fibre volume-fraction, V_f, of the order of 60%, with which this communication will deal, it has been suggested that the upper bound of compressive strength is equal in magnitude to the tensile strength. Ewins [1], Purslow and Collings [2], Kelly [15], Ewins and Ham [3], Collings [4] and Hancox [5] have postulated a shear-initiated fibre failure mechanism for CFRP failure in uniaxial tension and compression.

Earlier analyses involving buckling of lamellae (representing fibres) were introduced by Rosen [8]. His "shear instability" within the matrix criterion for the compressive strength,

$$\sigma_c = \frac{G_m}{1 - V_f}, \tag{1}$$

where G_m is the shear modulus of the matrix, predicts a value of $\sim 4\,\text{GN}\,\text{m}^{-2}$ for 60% V_f CFRP, which is 2 to 4 times the reported results. It should be added that, if a similar analysis were to be applied to a metal matrix composite, the compressive strength should be some 50 times higher than that of CFRP; however, measured values of CFR nickel are comparable to those of CFRP [16].

The "kinking–collapse" failure mechanism for composites was initially suggested by Argon [10], who attributed it to the misalignment of fibres relative to the compressive axis. Kinking has been observed in numerous composites and studied in uniaxial compression of uniaxially aligned CFRP by Chaplin [17]. Weaver and Williams [7], using only 36% V_f CFRP, also investigated its behaviour under superposed hydrostatic pressure. They observed a transition at ~110 $MN\,m^{-2}$ superposed pressure from a "splitting" to a "kinking" failure mode. Kinking in CFRP has also been observed in flexural specimens [18].

2. Experimental procedure

Our experiments were performed on samples machined from a pultruded rod 8 mm in diameter obtained from Courtaulds Ltd. The pultrusion contained 60% V_f of Grafil A-S (Type III carbon fibres) in an epoxy resin matrix.

Longitudinal compression test specimens were fabricated to the "dog-bone" design illustrated in Fig. 1a. Constraints were placed on this specimen design by the size and shape of the testing assembly in the pressure vessel. In-plane shear specimens were of similar design to that of Loveless and Ellis [19], but were fitted with aluminium end tabs (see Fig. 1b), to aid alignment within the pressure vessel testing rig.

It was not practicable with our pressure rig to test specimens made according to the Royal Aircraft Establishment (RAE) design [20]. To allow comparisons therefore, samples (from another batch, Batch B, of CFRP) were made according to our and RAE (Fig. 1c) designs and tested at atmospheric pressure.

Mechanical testing was performed on a Hedeby Universal tester fitted with a Coleraine pressure cell. Both specimen types were loaded in axial compression at a rate of 0.1 $mm\,min^{-1}$, at atmospheric and at superposed hydrostatic pressures extending to 300 $MN\,m^{-2}$. 'Plexol', a synthetic diester, served as the pressuring medium. Loads were measured on an (external) B.L.H. semiconductor load cell. The load monitored in pressure tests included frictional forces on the loading and dummy pull-rods. As these forces were much lower than the axial loads on the specimens, they were determined before and after a specimen was strained and substracted from the recorded force to give the superposed compressive load.

Specimen failure surfaces were examined on an ISI Super III scanning electron microscope. Some samples were mounted in polyester resin, sectioned and polished parallel to the fibre direction for observation by reflection optical microscopy. The same resin was also used to encapsulate several compression specimens prior to testing at atmospheric pressure to allow the failure process to be interrupted and the microstructure examined. Photomicrographs of sectioned samples were taken on a Zeiss Ultraphot II optical microscope.

3. Results

3.1. RAE type specimens

The compressive strength, calculated from the maximum load, for Batch B, was found to be $1.30 \pm 0.07\,GN\,m^{-2}$. Failure was catastrophic with the samples separating into two portions along a line approximately 30° to the fibre axis. Closer examination, involving sectioning of the fractured parts parallel to the fibre axis prior to microscopic

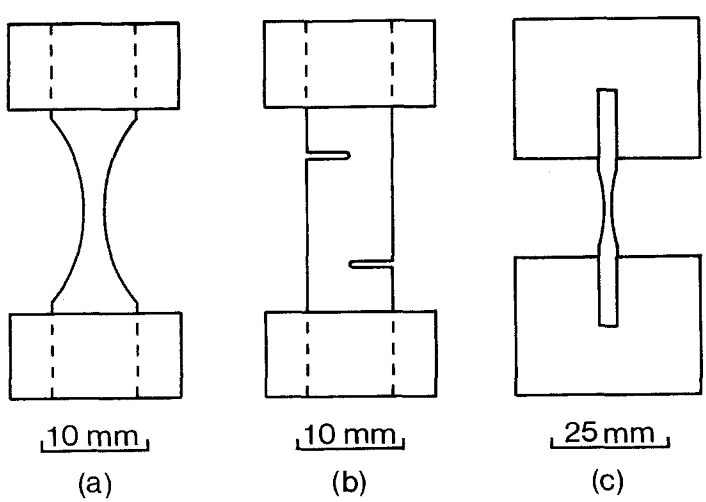

Figure 1 Test specimens used in this investigation, (a) "dog-bone" compressive, (b) in-plane shear and (c) RAE compressive (rectangular).

examination, revealed that the failure process involved kinking with eventual separation along one (or both) of the kink boundaries, as seen in Fig. 2a for example.

3.2. "Dog-bone" Specimens

Atmospheric pressure data were similar to those for RAE type specimens; compressive strength for the same batch of material (Batch B) was $1.33 \pm 0.15\,GN\,m^{-2}$. The failure mode was again similar and is illustrated in Fig. 2b for a Batch A specimen. Kinking was preceded by some longitudinal splitting from the reduced gauge length (see Fig. 3). For the Batch A material the atmospheric compressive strength was $1.50 \pm 0.14\,GN\,m^{-2}$. This increased apparently linearly with superposed hydrostatic pressure, H, (see Fig. 4) with a slope of about 0.6, up to $H = 150\,MN\,m^{-2}$; above this pressure the slope increased markedly to 3.2. Only in specimens tested up to the transition pressure was kinking preceded by longitudinal splitting. All failures, however, were associated with the propagation of kink bands and Fig. 2c illustrates the process for a specimen tested at a pressure of $250\,MN\,m^{-2}$.

Due to the catastrophic nature of the composite failure, only samples encapsulated in a transparent polyster resin could be unloaded at various stages of the process. Fig. 5a shows a partially formed kink band and the longitudinal splitting that preceded its formation in a specimen whose test was stopped immediately the applied load started to decrease. In Fig. 5b, taken at a higher magnification, it is seen that fibres ahead of the kink band have failed and that these fractures are generally perpendicular to the axis of loading. If specimens were unloaded at a later stage of the failure propagation process, conjugate kinks were observed. Fig. 6a illustrates a typically fully-developed kink with a conjugate kink formed perpendicular to it and the section. This micrograph can be compared to Fig. 6b (kindly provided by Mr R. J. Howard) which is of conjugate kinks in a CFR nickel composite tested in compression.

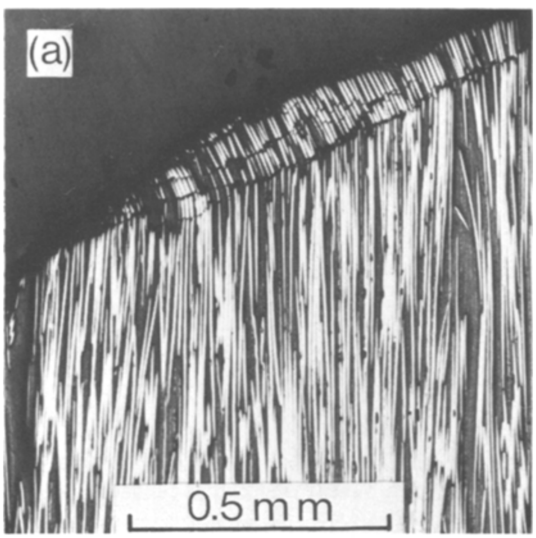

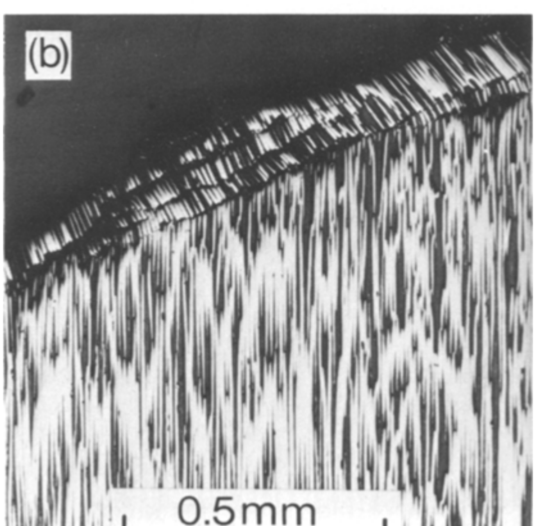

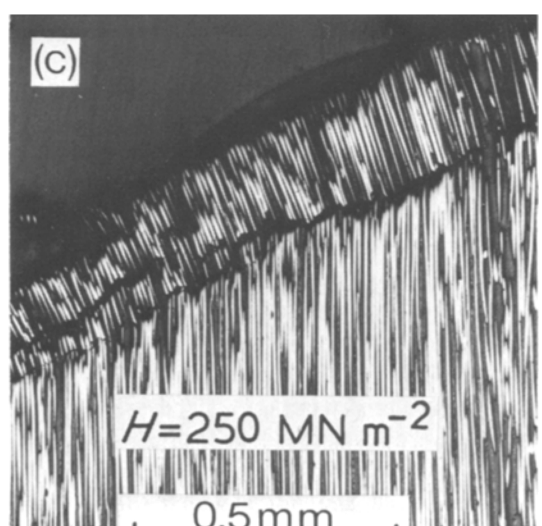

Figure 2 Kink bands in failed sectioned compressive CFRP specimens of (a) RAE and (b) and (c) "dog-bone" designs, at approximately 30° to the loading (and fibre) axis. Specimens (a) and (b) were tested at atmospheric pressure and (c) at $250\,MN\,m^{-2}$ superposed pressure.

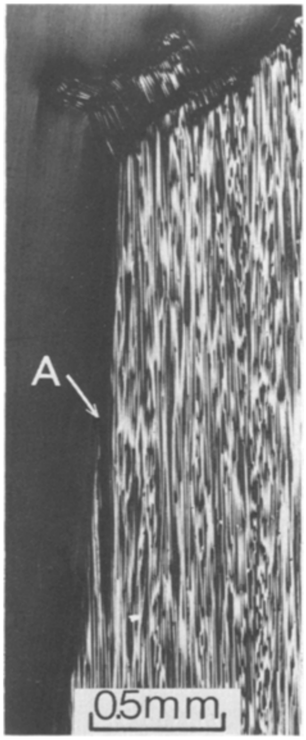

Figure 3 Sectioned compressive CFRP specimen showing longitudinal splitting from A, the end of the gauge length, and the group of fibres of the kink band which initiated fracture.

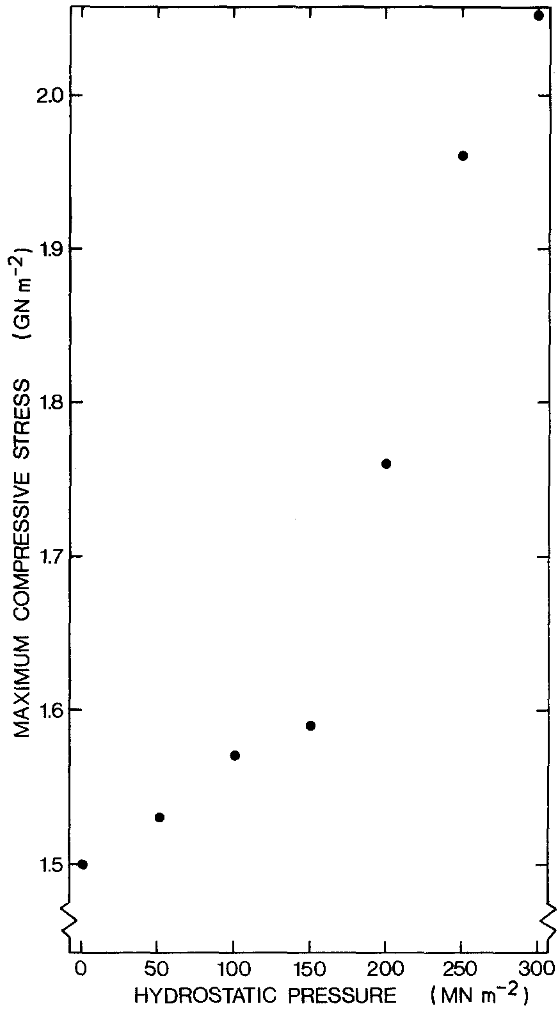

Figure 4 Maximum compressive stress for CFRP specimens tested in axial compression under superposed hydrostatic pressure.

3.3. In-plane shear specimens

Shear stength, calculated using the planar prospective (mid-plane) sheared area, is evaluated as 75 ± 2 MN m^{-2} at atmospheric pressure. This parameter is shown plotted as a function of superposed pressure in Fig. 7; "shear" failure, however, occurred only in specimens tested up to 150 MN m^{-2} pressure. Samples tested at higher pressures failed in a controlled manner with a gradual reduction in load by kink propagation from the tip of the cut-out notches. A typical failure is illustrated in Fig. 8 for a specimen tested at 300 MN m^{-2} superposed pressure.

4. Discussion

It has been recognised and pointed out, e.g., with reference to glass–epoxy composites by Chou, Stewart and Bader [14] that the compressive strength values for unidirectionally aligned fibrous composites can depend on the design of test fixtures. This discussion will be restricted therefore to the consideration of failure mechanisms in the specimens tested and not a search for a "true" compressive strength parameter, which might prove as elusive as the compressive upper yield stress in mild steel. The latter does not inhibit designers basing their calculations on the shear stress-controlled lower yield strength.

It is in polycrystalline metallic materials that lower yield stresses are generally equal in tension and compression and, if the tensile and compressive strengths of CFRP were equal, this would be consistent with a simple shear-stress operated mechanism of failure, as proposed by the RAE workers. Although the tensile strength of our material, 1.51 ± 0.07 GN m^{-2}, was the same as the compressive strength, 1.50 ± 0.14 GN m^{-2}, no such hypothesis is tenable once the results under pressure are considered. Shear-stress operated mechanisms are pressure independent, e.g. yield strength of many metals and alloys, and therefore

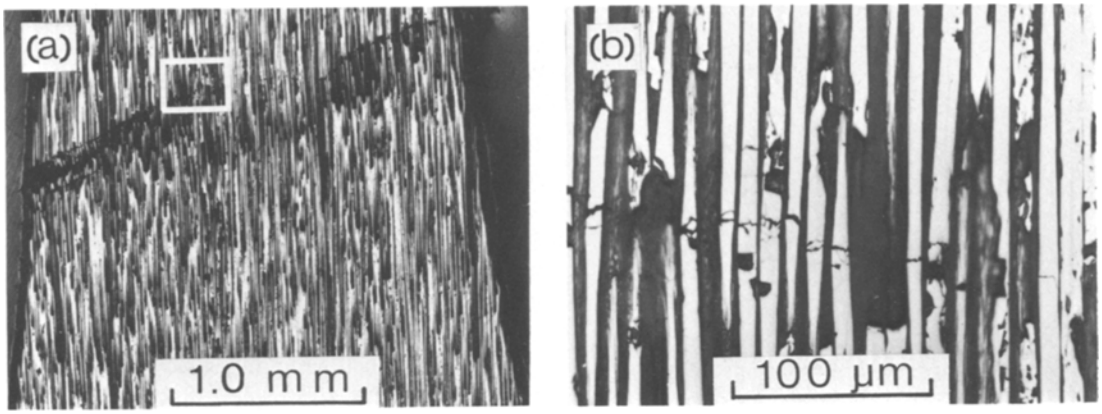

Figure 5 Micrographs of an encapsulated sectioned CFRP compressive specimen showing (a) longitudinal splitting and propagating kink bands (b) fractured fibres ahead of the kink band [marked with a rectangle in (a)].

for uniaxial compression the maximum principal compressive stress increases with increasing pressure with a slope of unity.

Whilst it could be argued this is so within the experimental error for CFRP (Fig. 4) with $H < 150\,\mathrm{NM\,m^{-1}}$ (the slope being approximately 0.6), it cannot for higher pressures, as the slope is approximately 3.2. It should be noted that results of similar tests on tensile specimens are complex [21], but that for CFRP beam specimens tested in bending in a pressure region where failure was uniquely by a tensile mechanism, data were consistent with a critical tensile stress criterion [18], as they were for a CFR nickel composite tested in tension under superposed pressure [21].

If it were argued that our compressive strength values lie below the "upper bound" of σ_c determined by fibre shear, it would be pointed out that (Type III) fibres in our specimens tested at 300 $\mathrm{MN\,m^{-2}}$ pressure supported shear *stresses* of about $1.5\,\mathrm{GN\,m^{-2}}$, rather higher than the supposed shear "strengths" of about $0.9\,\mathrm{GN\,m^{-2}}$ of Type I and II fibres reported by, e.g. Ewins and Ham [3]. Mechanisms dependent on the supposed shear-stress controlled failure of fibres in CFRP will therefore not be considered in relation to observed compressive failure behaviour.

Another model, due to Chaplin [17], attempts a fracture mechanics analysis and considers unstable "shear mode" failure (shear instability) from a notch. He suggests that the notch insensitive strength of CFRP may be due to inherent fibre weakness in shear, rather than the "theoretical" shear mode operating. He also argued earlier [11], when considering volumetric strains, that in the presence of a hydrostatic stress component, the expected effect would be an increase in compressive strength, which is qualitatively in agreement with our results.

This large pressure dependence of the compres-

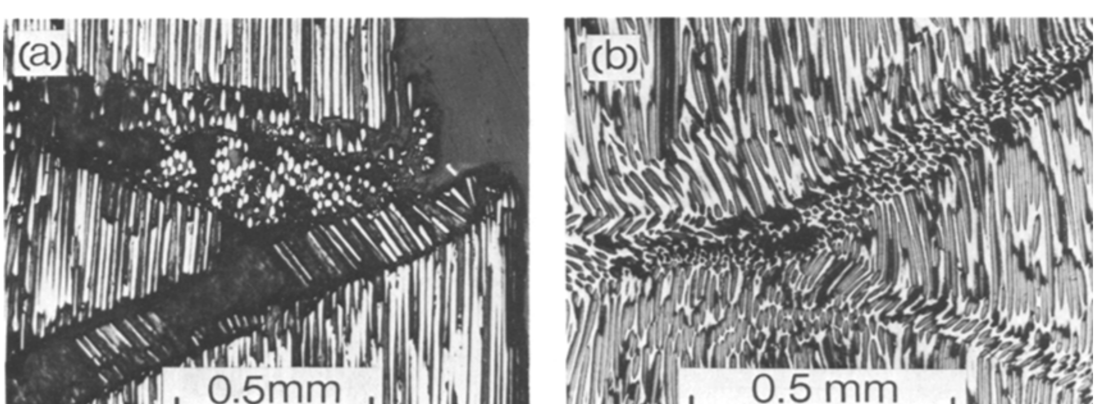

Figure 6 Conjugate kinks in specimens tested in axial compression for carbon fibre composites with (a) resin matrix and (b) nickel matrix.

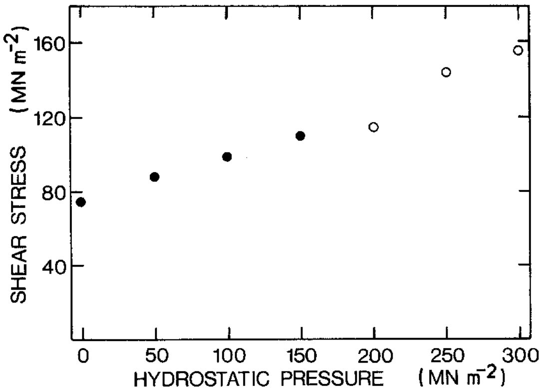

Figure 7 Maximum (interlaminar) shear stress for in-plane shear specimens tested under superposed hydrostatic pressure. Full symbols denote shear cracking failure mode.

sive strength of CFRP adds further criticism to any model dependent on the shear modulus of the matrix [8], which is only weakly pressure dependent [7]. Even if, as Lager and June [22] have suggested, an "influence factor" is incorporated into Equation 1, our data cannot be interpreted simply in terms of the properties of the matrix. Piggot and Harris [23], who carried out extensive experiments on composites of many different types of fibre in numerous polyester resin matrices, have also criticised this relation on the grounds that it does not predict the correct dependence on fibre volume-fraction.

Micrographic evidence, shown in Figs 2, 3, 5 and 6a however, clearly identifies the mode of failure in this material as kinking, involving microbuckling of fibres. Kinking has been observed in many systems under different loading conditions,

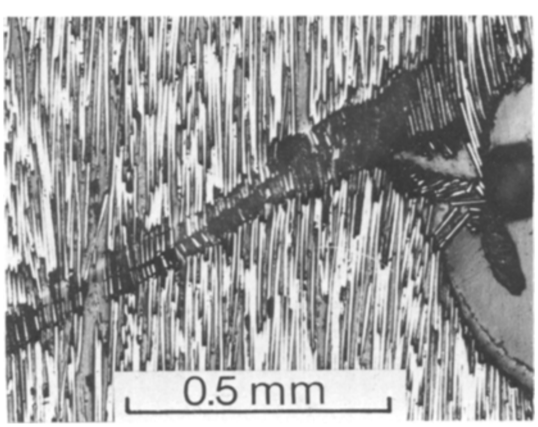

Figure 8 Kinking initiated by the "deep notch" of the CFRP in-plane shear-type specimen tested under superposed pressure of 300 MN m^{-2}.

but no clear failure criterion has yet emerged. Due to the catastrophic nature of the compressive failure process in CFRP, evidence of kink-controlled compressive failure appears to depend upon: (a) eventual separation occurring predominantly along one of the kink boundaries, (b) selecting and sectioning the portion of the failed specimen with the kink band, and (c) the fracture surfaces not being further damaged as they are driven together by the release of stored elastic strain energy and, perhaps, the testing machine.

Relevant microstructural observations were therefore made with encapsulated specimens which, when tested at atmospheric pressure, were under a small transverse compression due to the polyester capsule. The deformation of the specimen of Fig. 5 was apparently still linear when it was unloaded. Fig. 5b shows a group of fractured fibres ahead of the initiated kink band. It is suggested that this is a microbuckled group which failed by a tensile mechanism, as the fibre breaks are approximately perpendicular, and not at 45° to the fibre axis. Furthermore, as, on unloading, fractured and unfractured fibres appear straight, it would seem that the deformation preceding failure is recoverable. It is therefore suggested that a local surface condition initiates the first buckling and breakage of a group of fibres, which acts as the kink band which propagates by the buckling and failure of fibre groups ahead of it. The surface of tensile fibre breaks ahead of the band delineates the path of subsequent kink propagation. This mechanism appears to be the same as in specimens of similar CFRP, tested in simple and pure bending over different spans under superposed pressures [18], where failure was initiated by kinking on the concave beam surfaces and obeyed no simple or complex stress criterion of failure.

Weaver and Williams [7] have also tested CFRP (36% V_f) under superposed hydrostatic pressures. They reported longitudinal splitting in (cylindrical) specimens tested up to ~ 100 MN m^{-2} and kinking in all samples tested at higher pressures. The difference in atmospheric fracture mode to that reported here indicates the importance of V_f and specimen geometry with regard to failure mode as well as fracture strength; in our samples it appears that kinking in uniaxial compression was preceded by some longitudinal splitting. Their model for kinking was based upon Eulerian buckling of individual fibres; giving for the compression strength:

$$\sigma_c = \frac{\pi^2 E_f}{(l/K)^2}, \quad (2)$$

where E_f is the fibre modulus, K is the radius of gyration and l is the buckling length. Their values of l, evaluated at about 20 μm, are in good agreement with fractured fibre lengths, $\sim \frac{1}{2}l$.

Applying the analysis of Weaver and Williams to our data yields a value of l of about 70 μm and therefore kink band widths of the order of 35 μm. Observed values were, however, in the range 100 to 400 μm, which appears inconsistent with the Weaver and Williams model [7]. Examination of their micrographs indicates that their specimens failed in a progressive manner and therefore that the short fractured fibre lengths in their kink bands could well be an artefact of post-failure deformation, rather than relating to kink initiation.

Our values of strength can be interpreted in terms of elastic buckling of the fibres only if it is assumed that groups of fibres behave collectively. There is some evidence to support this simple assumption, for example in Fig. 3 a group of fibres of an overall diameter about 0.43 mm appears to have buckled as one unit. The predicted buckling length of this group, according to Equation 2 and using the composite modulus for E, is about 2.9 mm. In Fig. 3 it can be seen that the longitudinal splitting from the gauge diameter has effectively increased the gauge length from 1 to approximately 4 mm (half of which is illustrated in the figure) and this could behave as an "effective buckling length".

Let us now turn to the plane shear specimens, each of which can also be regarded as two notched compressive specimens (Fig. 1b), and first consider the pressure range extending up to about 150 MN m^{-2}. The failure at atmospheric pressure was by shear cracking at a (general) shear stress of 75 ± 2 MN m^{-2}. This shear stress at failure increased with increasing pressure (Fig. 7, slope approximately equal to 0.25) in a similar way to the yield strength of expoxides, indicating that this parameter controls the failure process. The higher value of shear stress at atmospheric pressure for the CFRP, i.e. about 75 compared to about 55 MN m^{-2} of the resin alone [24], probably reflects the higher actual failure area in the composite and can also be associated with the thin layers of the "adhesive" holding the CFRP tows.

At higher superposed pressures, however, the plane shear specimens behaved as notched compressive samples and therefore an attempt can be made to analyse their failure using the Chaplin Linear Elastic Fracture Mechanics model [17]. Chaplin has suggested that for large notches, beyond 4 mm in depth, as was the case with our specimens, compression fracture propagation can be stable (due to residual strength transmitted through the failed band) at a stress level of about 200 MN m^{-2}. At atmospheric pressure we observed, as sometimes did he, interlaminar shear crack propagation from the notches. At 150 MN m^{-2} superposed pressure, however, when compressive cracking was first seen in our notched specimens, nominal (maximum principal) compressive stress was 297 MN m^{-2} and increased to 514 MN m^{-2} at 300 MN m^{-2} superposed hydrostatic pressure. The superposed compressive stress, on the other hand, rose only from 146 to 214 MN m^{-2}, roughly in line with the strengthening observed in the resin alone [24]. Two tentative conclusions will be drawn from these observations. Firstly, it appears yet again that the compressive strength properties of CFRP are related to the strength, ductility and possibly toughness of the resin rather than its modulus. Transitions in mechanical behaviour of CFRP under superposed pressure have been observed at about 150 MN m^{-2} (not a significant stress for the fibres, but very large for the resin) for materials tested in compression, tension [21], bending [18] and interlaminar shear [18]. Secondly, under complex loading such as superposed hydrostatic pressure, the relevant stress parameter seems to be the superposed (or perhaps deviatoric) maximum stress or strain, which indicates that only a part of the stored elastic energy (perhaps the distortional) is available for fracture. This has important implications for cracking analyses also of ceramics [25] and polymers [24], where tensile cracking (perpendicular to the maximum tensile strain) has been observed when all the principal stresses, though unequal, were compressive.

Acknowledgements

The authors wish to acknowledge the support of the Science and Engineering Research Council, the provision of laboratory facilities by Professor D. Bijl and discussions with and comments on the manuscript by Dr C. R. Chaplin of the University of Reading.

References

1. P. D. EWINS, Royal Aircraft Establishment Technical Report Number TR-71217, (1971).
2. D. PURSLOW and T. A. COLLINGS, Royal Aircraft Establishment Technical Report Number TR-72096, 1972.
3. P. D. EWINS and A. C. HAM, Royal Aircraft Establishment Technical Report Number TR-73057, 1973.
4. T. A. COLLINGS, *Composites* **5** (1974) 108.
5. N. HANCOX, *J. Mater. Sci.* **10** (1975) 234.
6. K. KENDALL, *ibid* **11** (1976) 1267.
7. C. R. WEAVER and J. G. WILLIAMS, *ibid,* **10** (1975) 1323.
8. B. W. ROSEN, in "Fibre Composite Materials" edited by S. H. Bush (American Society for Metals, Metals Park, Ohio, 1965) p. 37.
9. L. B. GRESZCZUK, *AIAA.* **13** (1975) 1311.
10. A. S. ARGON, in "Treatise of Materials Science and Technology" Vol. 1, edited by H. Herman (Academic Press, London and New York, 1972) p. 79.
11. C. R. CHAPLIN, *J. Mater. Sci.* **12** (1977) 347.
12. A. G. EVANS and W. F. ADLER, *Acta Metall.* **26** (1978) 725.
13. P. D. EWINS and R. T. POTTER, *Phil. Trans. R. Soc. Lond.* **A294** (1980) 507.
14. T. W. CHOU, W. B. STEWART and M. G. BADER in "New Developments and Applications of Composites" edited by D. K. Wilsdorf and W. C. Hanigan, (Metallurgical Society of the AIME, 1979) p. 331.
15. A. KELLY, in "Composites Standards, Testing and Design" Proceedings of the National Physical Laboratory Conference, London, April 1974 (IPC Science and Technology Press, Guildford, 1974) p. 9.
16. A. S. WRONSKI and R. J. HOWARD in "High Pressure Science and Technology" edited by B. Vodar and Ph. Martenau (Pergamon Press, Oxford, 1980) p. 296.
17. C. R. CHAPLIN, Conference on Significance of Defects in the Failure of Fibre Composites, London, November 1979, (Institute of Physics, London), to be published.
18. T. V. PARRY and A. S. WRONSKI, *J. Mater. Sci.* **16** (1981) 439.
19. H. S. LOVELESS and J. H. ELLIS, *J. Test. Eval.* **5** (1977) 369.
20. P. D. EWINS, in "Composites, Standards, Testing and Design" National Physical Laboratory Conference, London, April 1974 (IPC Science and Technology Press, Guildford, 1974) p. 144.
21. A. S. WRONSKI, Proceedings of the Fourth International Conference on Fracture, Munich, 1973 (Verein Deutscher Eisenhüttenkute, Düsseldorf, 1973) p. II-332.
22. J. R. LAGER and R. R. JUNE, *J. Comp. Mater.* **3** (1969) 48.
23. M. R. PIGGOTT and B. HARRIS, *J. Mater. Sci.* **15** (1980) 2523.
24. A. S. WRONSKI and M. PICK, *ibid,* **12** (1977) 28.
25. A. S. WRONSKI and R. J. HOWARD, in "High Pressure Science and Technology" edited by B. Vodar and Ph. Marteau (Pergamon Press, Oxford, 1980) p. 296.

Received 21 July
and accepted 18 August 1981